INTERPRETATION OF THE OPTIMAL FREQUENCY FOR SKIN FRICTION DRAG REDUCTION WITH SPANWISE WALL-OSCILLATION CONTROL

A. Yakeno, Y. Hasegawa and N. Kasagi

Department of Mechanical Engineering, The University of Tokyo
Hongo 7-3-1, Bunkyo-ku, Tokyo 113-8656, JAPAN
yakeno@thtlab.t.u-tokyo.ac.jp

Abstract

Through a series of direct numerical simulation of turbulent channel flow, we investigate the mechanisms of drag reduction by the spanwise wall-oscillation. We focus on the quasi-streamwise vortex and associated Reynolds stress near the wall by employing a conditional sampling technique. We identify two major mechanisms to reduce the Reynolds stress near the wall. The first is the weakening of Q2 event, which is always observed with a specific time delay from the moment when the wall motion starts to counteract to the vortical motion adjacent to the wall. The second is the suppression of the streamwise vortex and associated Reynolds stress, which results from the tilting of the vortex caused by the periodic Stokes layer induced. It is also found that, in the quadrant analysis of Reynolds stress, the close correlation of occurrence of Q2 and Q4 events around the quasi-streamwise vortex is substantially deteriorated by the spanwise wall oscillation control. The optimal control frequency of wall-oscillation control is determined as a tradeoff between the two limiting factors. Namely, the oscillation frequency should be low enough so that the Stokes layer develops sufficiently thick to affects the near-wall vortex, while it should be high enough to avoid the enhancement of a streamwise vortex due to spanwise titling.

1 Introduction

Spanwise wall-oscillation control (Jung, *et al.*, 1992) is known for its simplicity to achieve considerable friction drag reduction in wall turbulence. Although the drag reduction mechanism has been extensively discussed in the last decade, there is few satisfactory explanation about its optimal oscillation period of $T^+ \sim 100$. The structural change of streaks around a streamwise vortex under the control has been reported in previous studies (Baron and Quadrio, 1996; Choi *et al.*, 2002; Yakeno, *et al.*, 2009). Coleman *et al.* (1996) explain the optimal frequency on a basis of the Stokes layer, i.e., the solution of the second Stokes problem. In spite of these extensive studies, it is still unclear how the coherent structures respond to the Stokes layer at each phase and how such structural modifications contribute to the overall drag reduction. In the present study, we employ a conditional sampling technique to detect vortex cores in order to extract essential features of the near-wall coherent structures at different oscillation phases. By analyzing the phase-averaged flow field, we discuss the quantitative contribution of each of the structural modifications to the overall skin friction based on FIK identity, which gives theoretically the componental dynamical contribution to the skin friction coefficient (Fukagata *et al.*, 2002). Finally, we try to seek a physical interpretation for the optimal oscillating period.

2 Computational Methods

We consider a fully developed turbulent channel flow between two parallel walls. The computational scheme is the same as that is described in Satake and Kasagi (1996). All simulations are performed under a constant pressure gradient so that the friction Reynolds number is kept constant at $Re_\tau = 150$. The computational domain is $2.5\pi\delta \times 2\delta \times \pi\delta$ in the streamwise, wall-normal and spanwise directions, respectively. The numbers of grids are $(N_x, N_y, N_z) = (64, 128, 64)$, while the spatial resolutions are $\Delta x^+ = 18.4, \Delta y^+ = 0.189 \sim 5.70$ and $\Delta z^+ = 7.36$. Superscript + represents a value in the viscous wall unit. As for the control input, we impose a spanwise sinusoidal velocity component, $w^+ = W_0^+ sin\phi$, on the two parallel walls, where $\phi = 2\pi t^+/T^+$ is the phase of wall oscillation. The wall velocities at the two walls are in phase. The control parameters to be prescribed are the amplitude W_0^+ and the oscillation period T^+. In this paper, the former is fixed at $W_0^+ = 7.0$ since this value brings the maximum energy saving rate (Yakeno *et al.*, 2009), while the latter is changed as $T^+ = 16, 50, 75, 125, 200, 250$ and 500.

3 Fundamental Statistics

Identity equation for skin friction coefficient

With a periodic wall-oscillation imposed, the resultant velocity field can be considered as a superposition of time mean $\bar{u}_i$, periodic $\tilde{u}_i$, and irregularly fluctuat-

ing u_i" components.

$$u_i = \bar{u}_i + \tilde{u}_i + u_i". \quad (1)$$

The time-mean streamwise velocity $\bar{u}^+$ is shown in Figure 1. The streamwise velocity becomes the largest at $T^+ = 75$ among the cases tested, i.e., $T^+ = 16, 75, 125$ and 250. Note that the present optimal oscillation period is smaller than $T^+ \sim 100$, which has been reported in previous studies (Quadrio and Ricco, 2004; Yakeno *et al.*, 2009). If we use the friction velocity u_τ of controlled flow, the optimal period in the previous results coincides with the present one.

The phase change of root-mean-squre periodic velocity components of $\tilde{u}^+, \tilde{v}^+$ and $\tilde{w}^+$ are shown over the half priod in Figure 2. It should be noted that $\tilde{v}^+$ is analytically zero due to the continuity equation. In addition, the oscillation period of $\tilde{u}^+$ is a half of that of $\tilde{w}$. This is due to the symmetric property of the flow with respect to the spanwise direction. The component $\tilde{w}^+$ represents the Stokes layer (Schlichting, 1968; Ma *et al.*, 1999). The thickness of the Stokes layer is given as $\delta_s^+ = \sqrt{T^+/\pi}$, which is defined as a location where the amplitude becomes W_0^+/e. Thus, the thickness δ_s^+ solely depends on the control time period T^+. When the control frequency is high ($T^+ = 16$), the Stokes layer thickness is small, while it is low ($T^+ = 125$ or 250), the layer becomes thicker. The distribution of $\tilde{w}^+$ is essentially represents the Stokes layer on an oscillating wall, but the small $\tilde{u}^+$ component suggests slight deviation from the exact analytical solution in Figure 2.

In the case where the friction Reynolds number is kept constant with a constant pressure gradient, FIK identity (Fukagata *et al.*, 2002) is rewritten for representing the bulk mean velocity $\bar{u}_b^+$ as:

$$\bar{u}_b^+ = \frac{Re_\tau}{3} - \int_0^{Re_\tau} \left(1 - y^+/Re_\tau\right)\left(-\overline{u'v'}\right)dy^+ \quad (2)$$

The Reynolds shear stress arises from two parts, i.e., $-\bar{\tilde{u}}\bar{\tilde{v}}$ and $-\overline{u"v"}$ by using the periodic decomposition (Equation (1)). The former one is always zero since owing to the continuity. Therefore, we can consider the contribution of Reynolds shear stress near the wall as $-\overline{u"v"}$ only. Hence, the increase in the mean streamwise velocity in Figure 1 is found due to the decrease in $-\overline{u"v"}$. The random Reynolds shear stress $-\overline{u"v"}^+$ becomes the smallest at $T^+ = 75$ as shown in Figure 3. The suppression of Reynolds stress near the wall significantly increases the bulk mean velocity $\bar{u}_b^+$ as implied by Equation (2).

Quadrant analysis of Reynolds shear stress

The instantaneous Reynolds stress product is classified into four quadrants of Q1 $\sim$ Q4 on the hodograph plane depending on the signs of $u"$ and $v"$. Among these events, Q2 event corresponds to a low-speed fluid moving upward, i.e., $u" < 0$ and $v" > 0$,

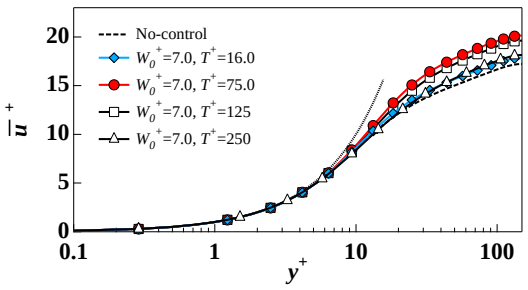

Figure 1: Time-mean streamwise velocity $\bar{u}^+$ in controlled flows.

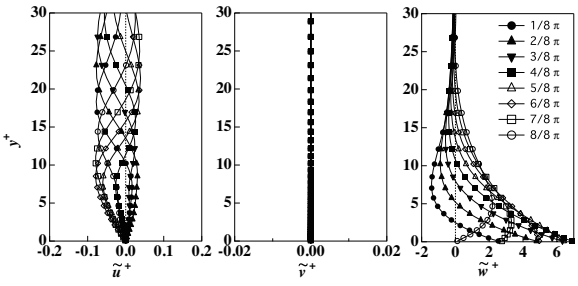

Figure 2: Phase change of $\tilde{u}^+, \tilde{v}^+$ and $\tilde{w}^+$ at $T^+ = 125$.

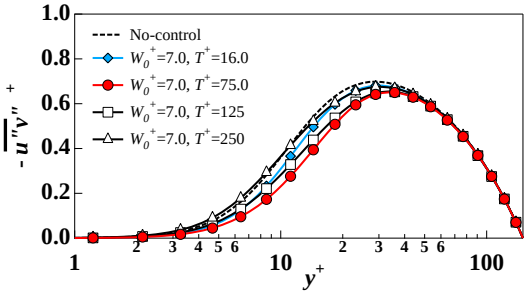

Figure 3: Reynolds shear stress $-\overline{u"v"}^+$ in controlled flows.

while Q4 event a high-speed fluid moving downward, i.e., $u" > 0$ and $v" < 0$. The quadrant contributions of Reynolds stress to $\bar{u}_b^+$ are shown in Figure 4 for different oscillation periods. The Q2 and Q4 events of the weighted Reynolds stress are decreased at all cases so that the drag is reduced considerably.

The Q2 and Q4 contributions for $\bar{u}_b^+$ are shown in Figure 5. The weighted Q2 and Q4 are close to the uncontrolled one at $T^+ = 16$. On the other hand, at $T^+ = 75, 125$, and 250, they increase with the control time period. However, this is not the case for Q2 event when the position is far from the wall. Basically Q2 and Q4 events occur at the same time around a streamwise vortex and they should have strong correlation. However, when the spanwise oscillation is imposed, the correlation is broken. It would be interesting to analyze further the observed change of near-wall structures with regard to Q2 and Q4 events.

4 Conditional Sampling

Coherent structures such as a quasi-streamwise vortex and low- and high-speed streaks are well established in near-wall turbulence (Robinson *et al.*, 1990). They are considered as main dynamical elements to generate the Reynolds shear stresses and enhance the drag. In order to investigate the effect of spanwise wall oscillation on the coherent structures, we obtain the conditionally averaged flow field around a vortex. First, we detect locations where the second invariant Q^+ of the deformation tensor is smaller than -0.04 in the region of $y^+ = 10 \sim 20$ at each phase. We define a vortex center at (x_c^+, y_c^+, z_c^+). In order to take into account the rotating direction of streamwise vortices, we choose only vortices of which vorticity ω_x is positive. Next, we ensemble-average the local three velocity components and the Reynolds shear stress around the vortex core over the sampling domain of $\Delta x^+ = x^+ - x_c^+ = -500 \sim 500, y^+ = 0 \sim 40$, and $\Delta z^+ = z^+ - z_c^+ = -40 \sim 40$. The conditionally averaged flow field and Reynolds shear stress in the uncontrolled case are shown in Figure 6. It is reconfirmed that strong Q2 and Q4 events are associated with a streamwise vortex.

Streak modification due to the induced spanwise velocity

Conditionally-averaged velocity vectors and Reynolds shear stress around a streamwise vortex in the y-z plane are shown in Figure 7. First, in the case of a comparatively low control-frequency (T^+=250), it is observed that Q2 event is drastically decreased at around $\phi = 4/8\pi$, which is about t^+=30 after the time instant when the spanwise wall motion starts to oppose the rotating direction of a streamwise vortex. Second, it is interesting to note that the vortical motion and associated Reynolds shear stress are considerably suppressed when the vortex-rotating direction coincides with the wall motion at $\phi = 12/8\pi$ in the same case. The vortical motion and associated Q4 event become close to those of uncontrolled flow at $\phi = 8/8\pi$ in spite of the counteracting wall velocity in Figure 7.

Top-views of a vortex and associated flow field are shown in Figure 8. The contour represents the streamwise velocity fluctuation u". In this Figure, the low-speed streak is suppressed at $\phi = 6/8\pi$ in the case of T^+=75, or $\phi = 4/8\pi$ in the case of T^+=250. The Q2 event of the Reynolds stress basically occurs within the low-speed streaks near the wall. Therefore, the suppression of Q2 event we observe in Figure 7 is caused by weakened low-speed streak. Next, it is known that the quasi-streamwise vortex in the uncontrolled flow is slightly tilted in the spanwise direction due to two counteracting driving effects. One is the streamwise mean shear (d/dy^+) and the other is the mutual induction caused by vortex-overlapping (Jeong, *et al.*, 1997). In Figure 8, the tilting angle of coherent structures is significantly affected by the spanwise induced velocity.

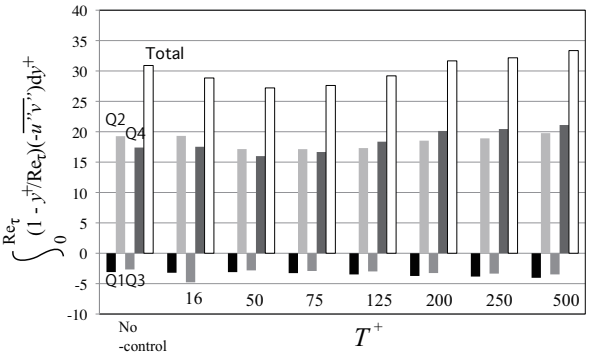

Figure 4: Quadrant contributions of the weighted Reynolds shear stress $-\overline{u"v"}$ of controlled flows.

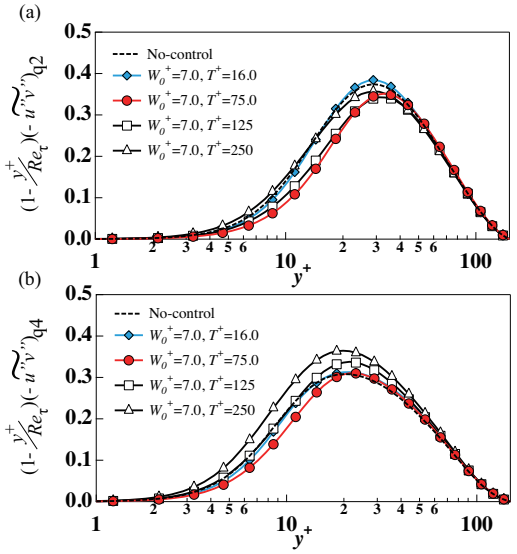

Figure 5: (a) Q2 and (b) Q4 compinents of the weighted Reynolds shear stress in controlled flows.

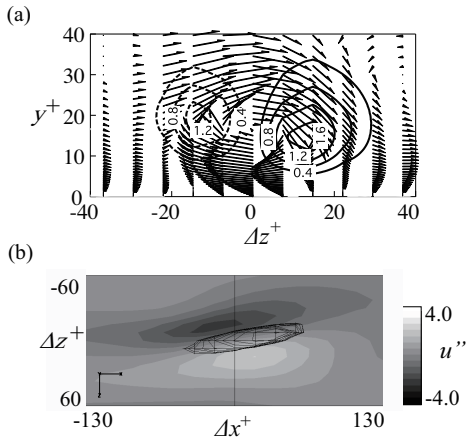

Figure 6: Conditionally-averaged flow structure around the vortex in the (a) $y-z$ plane and (b) $x-z$ plane (uncontrolled case, $\omega_x > 0$). In figure (a), dotted lines represent Q2 event and solid ones represent Q4 event . Velocity vectors are $(v", w")$. In figure (b), contour is $u"$ and black lines at the center denotes a streamwise vortex, with an iso-surface of $Q^+ = -0.013$

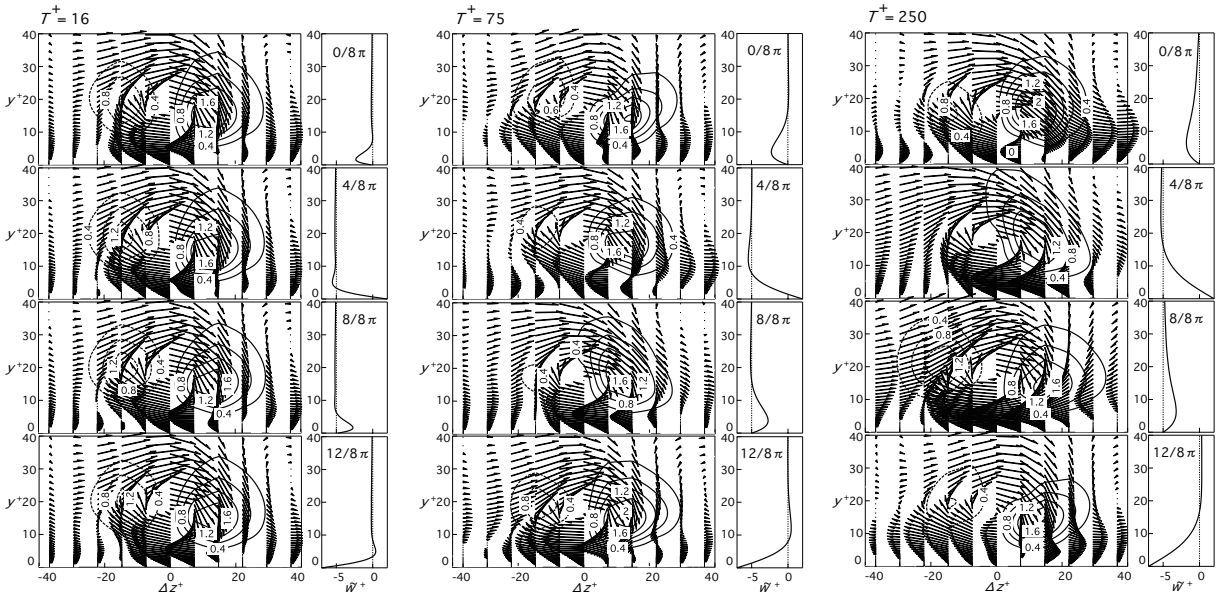

Figure 7: Conditionally-averaged flow structure around a vortex in y-z plane ($T^+ = 16, 75$ and 250, $\omega_x > 0$). Lines and vectors are noted in Figure 6.

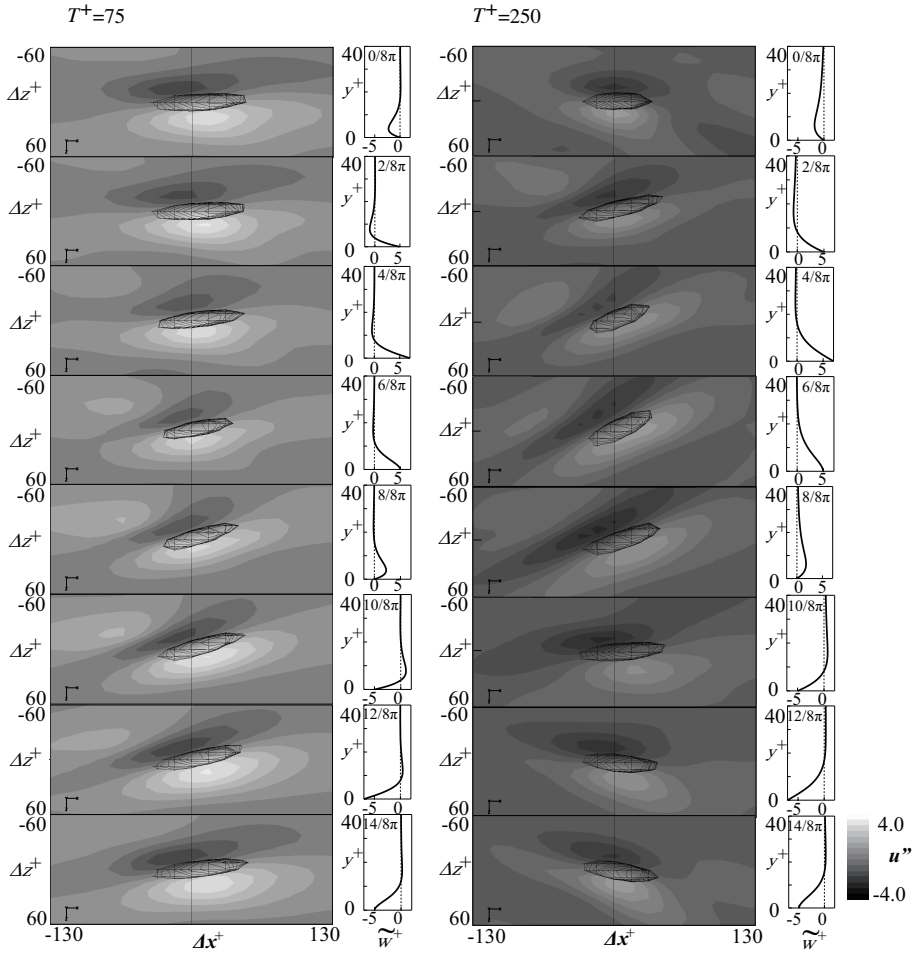

Figure 8: Conditionally-averaged flow structure around a vortex in x-z plane ($T^+ = 75$ and 250, $\omega_x > 0$). Contour represents u" and black lines at the center denotes a streamwise vortex, with an iso-surface of $Q^+ = -0.013$.

Tilting of a streamwise vortex and its maintenance

The mean streamwise component of pressure-strain $\overline{p"\partial u"/\partial x}$ is responsible for the transfer of kinetic energy $\overline{u"^2}$ to $\overline{v"^2}$ and $\overline{w"^2}$. The pressure-strain in the transport equation of $\overline{u"^2}$ is usually negative in turbulent shear flows (Tennekes and Lumley, 1972). Jeong, *et al.* (1997) suggest that the tilting of vortex is responsible for negative $\overline{p"\partial u"/\partial x}$ within the structure, since $p"$ is negative within the vortex and the tilting of streamwise vortex produces negative $\partial u"/\partial x$. The phase-averaged streamwise component of pressure-strain is shown in Figure 9. When the spanwise tilting angle is increased, the vortex obtains more energy from the streamwise velocity so that its motion is enhanced (see, $\phi = 6/8\pi$-$8/8\pi$). In contrast, when the streamwise vortex is tilted to the opposite direction, it is weakened (see, ϕ =$12/8\pi$-$14/8\pi$ and $0/8\pi$).

In order to discuss quantitatively the tilting effect to the vortex, we calculate the tilting angle and the integral of weighted Reynolds stress, Q2 and Q4, over the whole sampling domain around a vortex as shown in Figure 10. It is found that both Q2 and Q4 events significantly change depending on the phase ϕ, except for the case of small oscillation period $T^+ = 16$. The tilting angle has strong correlation with the weighted Q4 value, while the phase change of Q4 event is directly related to the enhancement or suppression of the streamwise vortex. Figure 11 shows the phase dependency of the volume integral of a pressure-strain term around a vortex center and the tilting angle of an ensemble averaged streamwise vortex. There is a strong correlation between these two values. In conclusion, the vortex is tilted in the spanwise direction by spanwise induced-velocity and the pressure-strain term is affected by the tilting angle.

Interpretation of the optimal control frequency

With increasing the control period T^+, the Q2 and Q4 is more pronounced. The tilting has a strong correlation with Q4 value in Figure 10. In contrast, the contribution of Q2 event shows entirely different behavior. During ϕ = 0-π in the case of $T^+ = 250$, Q2 is drastically decreased when the spanwise control input opposes to the vortex-induced motion. If we focus on the case of high control frequency ($T^+ = 16$), this suppression of Q2 event doesn't occur. The tilting force does not work because the Stokes layer remains thin. On the other hand, if the control frequency is low ($T^+ = 250$), the Q2 becomes larger after $\phi = \pi$ comparatively. Generally, the Q2 and Q4 events should have strong correlation due to the streamwise vortex. However, when the oscillation time period is long, the pressure-strain term becomes larger after $\phi = \pi$ and the Q2 event is considerable for the total friction drag. In conclusion, the optimal time period for drag reduction should be large so that the Stokes layer affects a streamwise vortex to suppress Q2 event, but small enough to prevent the enhancement of streamwise vortex caused by the spanwise titling.

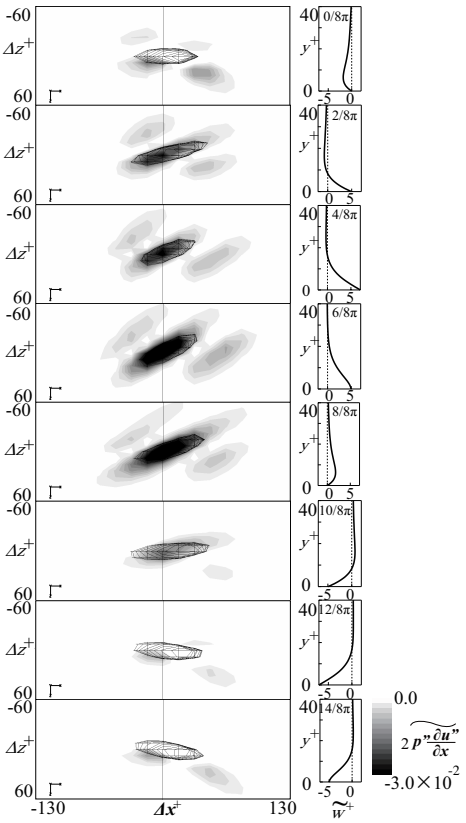

Figure 9: Conditionally-sampled flow structure around a vortex core at $T^+ = 250$. Contour represents $2(\widetilde{p"\partial u"/\partial x})$ and a black-lined structure represents an iso-surface of $Q^+ = -0.013$.

5 Conclusions

In order to obtain better understanding of the fundamental mechanisms of drag reduction caused by the spanwise wall oscillation, we carry out a series of direct numerical simulation of low-Re fully-developed turbulent channel flow at a constant pressure gradient. By employing a conditional sampling technique, we analyze the phase change of the turbulent flow structures such as the quasi-streamwise vortex and streaky structure, which exhibit marked modification due to the effect of the periodic Stokes layer formed by the control. The following conclusions are derived:

1. The two major mechanisms of reducing the Reynolds stress near the wall are identified. The first is the weakening of Q2 event, which is always observed with a specific time delay from the moment when the wall motion starts to counteract to the vortical motion adjacent to the wall. The second is the suppression of the streamwise vortex and associated Reynolds stress, which results from the tilting of the vortex caused by the Stokes layer induced.

2. It is found that, in the quadrant analysis of Reynolds stress $-\overline{u"v"}$, the close correlation of occurrence of Q2 and Q4 events around the quasi-

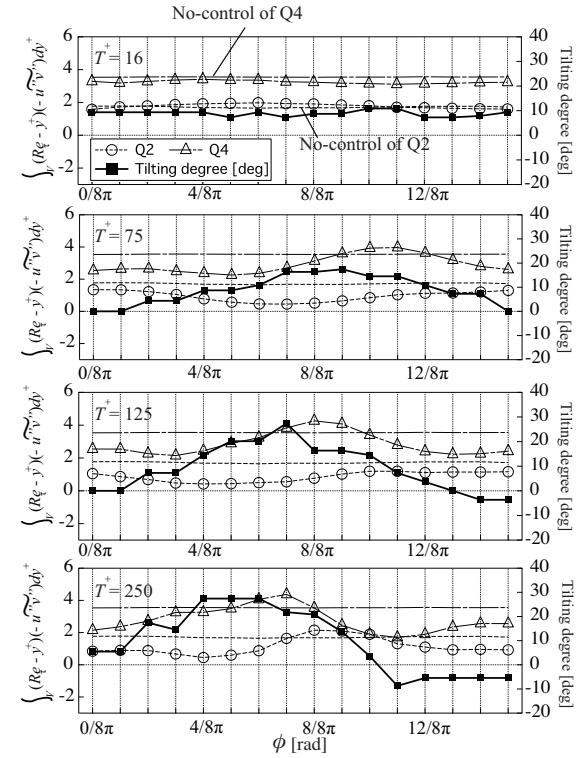

Figure 10: Phase dependency of an integral of the weighted Q2 and Q4 events (left vertical axis), and the tilting angle (right vertical axis).

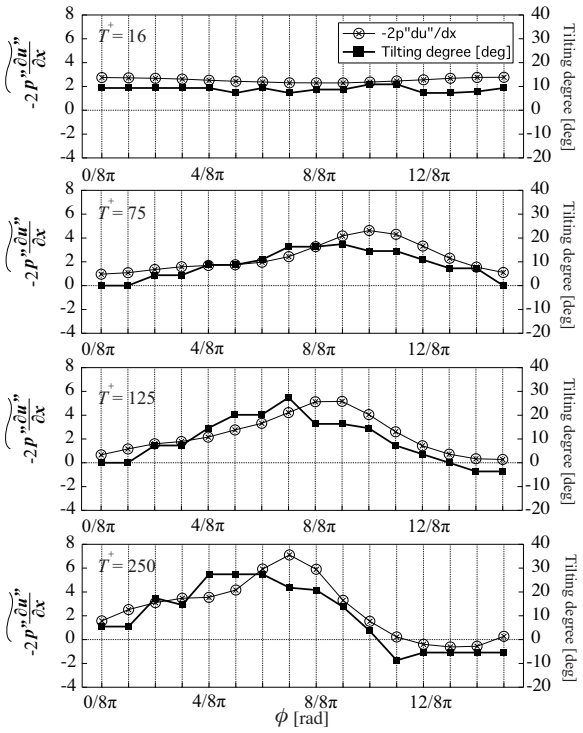

Figure 11: Phase dependency of a volume integral of $-2(\widetilde{p"\partial u"/\partial x})$ (left vertical axis) and the tilting angle (right vertical axis).

streamwise vortex is appreciably deteriorated when the spanwise wall oscillation control is imposed.

3. The optimal control frequency of spanwise wall-oscillation control is determined as a tradeoff between the two limiting factors. Namely, the oscillation frequency should be low enough so that the Stokes layer develops sufficiently thick to affects the near-wall streamwise vortex, while it should be high enough to avoid the enhancement of a streamwise vortex due to spanwise titling.

Acknowledgments

This work is supported through the Grant-in-Aid for Scientific Research (A) (No.20246036) by the Ministry of Education, Culture, Sports, Science and Technology (MEXT).

References

Baron, A. and Quadrio, M. (1996), Turbulent drag reduction by spanwise wall oscillations, *Applied Scientific Research*, Vol. 55, pp. 311-326.

Choi, J. I., Xu, C. X. and Sung, H. J. (2002), Drag reduction by spanwise wall oscillation in wall-bounded turbulent flows, *AIAA Journal*, Vol. 40, No. 5, pp. 842-850.

Coleman, G. N., Kim, J. and Le, A-T. (1996), A numerical study of three-dimensional wall-bounded flows, *Int. J. Heat Fluid Flow*, Vol. 17, pp. 333-342.

Filippone, A. (2000), Data and performances of selected aircraft and rotorcraft, *Progress in Aerospace Science*, Vol. 36, pp. 629-654.

Fukagata, K., Iwamoto, K. and Kasagi, N. (2002), Contribution of Reynolds stress distribution to the skin friction in wall-bounded flows, *Phys. Fluids*, Vol. 14, pp. L73-L76.

Jeong, J., Hussain, F., Schoppa, W. and Kim, J. (1997), Coherent structures near the wall in a turbulent channel flow, *J. Fluid Mech.*, Vol. 332, pp. 185-214.

Jung, W., Mangiavacchi, N. and Akhavan, R. (1992), Suppression of turbulence in wall-bounded flows by high frequency spanwise oscillations, *Phys. Fluids*, Vol. 6, pp. 335-359.

Ma, B., Von Doorne, C. W. H., Zhang, Z. and Nieuwstadt, F. T. M. (1999), On the spatial evolution of a wall-imposed periodic disturbancein pipe poiseuille flow at Re=3000. Part 1. Subcritical Disturbances, *J. Fluid Mech.*, Vol. 398, pp. 181-224.

Quadrio, M. and Ricco, P. (2004), Critical assessment of turbulent drag reduction through spanwise oscillations, *J. Fluid Mech.*, Vol. 521, pp. 251-271.

Robinson, S. K., Kline, S. J. and Spalart, P. R. (1990), Quasi-coherent structures in the turbulent boundary layer, *Near Wall Turbulence*, pp. 218-247.

Satake, S. and Kasagi, N. (1996), Turbulence control with wall-adjacent thin layer damping spanwise velocity fluctuations, *Int. J. Heat and Fluid Flow*, Vol. 17, pp. 343-352.

Schlichting, H. (1968), Boundary-layer Theory, McGraw-Hill, New York, pp.93-95.

Tennekes, H. and Lumley, J. L. (1972), A First Course in Turbulence, MIT press.

Yakeno, A., Hasegawa, Y. and Kasagi, N. (2009), Spatio-temporally periodic control for turbulent friction drag reduction, *TSFP6*, Vol. 2, pp. 599-603.